



# Microstructure and Electrical Conductivity of Atmospheric Plasma-Sprayed LSM/YSZ Composite Cathode Materials

Chao Zhang, Wen-Ya Li, Hanlin Liao, Chang-Jiu Li, Cheng-Xin Li, and Christian Coddet

(Submitted February 26, 2007; in revised form June 8, 2007)

Yttria stabilized zirconia and lanthanum strontium manganate (YSZ/LSM) have been employed to fabricate the composite cathode layer for solid oxide fuel cells (SOFCs). In the present study, the YSZ/LSM composite coating was deposited by atmospheric plasma spray (APS) using the mechanical blending LSM and YSZ with ratios of 50:50, 40:60, and 20:80 wt.%. The electrical conductivity of the composite coating was measured by the means of direct current (DC) measurement in the temperature range of 500–900 °C. The electrical conductivity of the YSZ-50%LSM coating ranged from 2.17 to 3.60 S/cm along the direction parallel to the coating surface at the temperature range. For the same specimen, the electrical conductivity perpendicular to the plane is less than one-tenth of that in the plane. The anisotropy of the electrical conductivity is attributed to the phases of different properties in the composite coating and the APS coating structure characteristics. The results also showed that the electrical conduction of the composite was strongly influenced by the YSZ content.

**Keywords** atmospheric plasma spraying, yttria stabilized zirconia, lanthanum strontium manganate, electrical conductivity

## 1. Introduction

Solid oxide fuel cells (SOFCs) have emerged as an alternative to conventional power generators, because of their environmentally friendly performance and high-conversion efficiency. For intermediate temperature SOFCs (IT-SOFCs), reducing the operation temperature of the SOFC system from 1000 to 600–800 °C attracts much attention for a significant cost reduction of systems by broadening the choice of compatible materials (Ref 1–3). Reduction of the system operating temperature requires new cathode materials with high-electrochemically cata-

lytic activity for oxygen reduction, as the oxygen reduction rate of conventional lanthanum strontium manganate (LSM) cathodes are significantly reduced below 800 °C.

The amelioration of lanthanum manganate ( $\text{LaMnO}_3$ ) may follow two pathways either by oxidizing the manganese cations, which increases the electrical conductivity, or by creating oxygen vacancies, which enhances the ionic conductivity. A few methods have been proposed: (i) selective B-site doping, which would increase the oxygen vacancy concentration (Ref 4), (ii) optimization of the microstructure, which would increase the number of triple phase boundary (TPB) lines (electrolyte/electrode/oxygen) and thus would ensure better surface exchange of oxygen and minimization of oxygen anion migration (Ref 5), and (iii) adding an ionic-conducting second phase (Ref 6, 7). It could be supposed that the third approach would combine the advantages of the first two, improving both composition and structure.

For high-temperature solid oxide fuel cells, when the thickness of electrolyte is reduced to a certain extent, the cathode polarization (electrochemical and diffusion polarization), becomes a bottleneck to improving the cell performance. Adding an ionic-conducting material, e.g. YSZ, to the conventional LSM cathode materials to form a composite cathode functional layer (CFL) between the electrolyte and conventional cathode layers could be a feasible method to decrease the electrochemical polarization of the cathode and has been investigated (Ref 8).

Although the LSM/YSZ composite cathode layer has attracted much attention from the investigators, the commonly used preparation technique was a screen-printing process (Ref 8–11). A post-heat treatment was needed and was limited to a temperature below 1250 °C to avoid the formation of lanthanum or strontium zirconates

This article is an invited paper selected from presentations at the 2007 International Thermal Spray Conference and has been expanded from the original presentation. It is simultaneously published in *Global Coating Solutions, Proceedings of the 2007 International Thermal Spray Conference*, Beijing, China, May 14–16, 2007, Basil R. Marple, Margaret M. Hyland, Yuk-Chiu Lau, Chang-Jiu Li, Rogerio S. Lima, and Ghislain Montavon, Ed., ASM International, Materials Park, OH, 2007.

**Chao Zhang, Chang-Jiu Li, and Cheng-Xin Li**, State Key Laboratory for Mechanical Behavior of Materials, Xi'an Jiaotong University, Xi'an, Shaanxi, China; and **Chao Zhang, Wen-Ya Li, Hanlin Liao, and Christian Coddet**, LERMPS, Université de Technologie de Belfort-Montbéliard, Site de Sévenans, Belfort Cedex 90010, France. Contact e-mail: hanlin.liao@utbm.fr.

(e.g.,  $\text{La}_2\text{Zr}_2\text{O}_7$ ,  $\text{Sr}_2\text{ZrO}_4$ ,  $\text{SrZrO}_3$ ). These phases usually decrease the cell performance due to their poor conductivity (Ref 12).

Plasma spray processing, especially atmospheric plasma spraying (APS) is a promising method to deposit cathode layer, as well as electrolyte layer, because of its high-deposition rate, cost effectiveness, and flexibility for automatic production. Some investigations have been conducted on pure LSM cathodes produced by APS processing (Ref 13, 14). Furthermore, with APS processing, post-thermal treatment is not needed and there is no possibility for the formation of lanthanum or strontium zirconates during preparation of the cathode. A few works has been reported that fabricated LSM/YSZ composite cathodes by plasma spraying (Ref 15-17). Electrical and electrochemical performances are two important capabilities of YSZ/LSM composite cathode. Although many electrochemical characterizations of YSZ/LSM cathode were reported (Ref 8-10, 16, 17), there is less investigation on electrical characterization of YSZ/LSM cathode, especially on the APS YSZ/LSM coating, e.g., on relationship between coating microstructure and coating electrical conductivity.

In this article, YSZ/LSM coatings were prepared by atmospheric plasma spray processing with different LSM/YSZ ratios. The electrical conductivity of the composite coatings along the directions both parallel and perpendicular to the coating surface was measured to investigate the relation between coating microstructure and coating electrical conductivity.

## 2. Experimental

### 2.1 Feedstock Materials

Commercially available 8 mol% YSZ (Marion Technologies, France) and  $\text{La}_{0.8}\text{Sr}_{0.2}\text{MnO}_3$  (Inframat Advanced Materials, USA) powders were used as feedstock materials. The morphologies of YSZ and LSM powders were shown in Fig. 1(a), (b). The powders size distribution was measured with a laser particle size analyzer (Mastersizer 2000, Malvern Instruments, UK) as shown in Fig. 2 and 3. The YSZ powder exhibited a  $D_{50}$  of 25.6  $\mu\text{m}$  and the LSM powder exhibited a  $D_{50}$  of 15.0  $\mu\text{m}$ . The YSZ and LSM powders were mixed to make YSZ-50%LSM, YSZ-40%LSM, and YSZ-20%LSM composite powders with

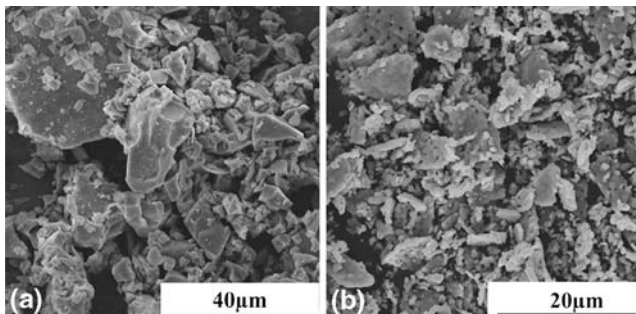


**Fig. 1** Feedstock powder SEM morphology: (a) LSM and (b) YSZ

respective YSZ:LSM weight ratios of 50:50, 60:40, 80:20 using a mechanical blending machine for 20 min.

### 2.2 Coating Preparation

LSM/YSZ composite coatings were deposited using APS system (PT-2000 with F4MB torch, Sulzer Metco AG, Switzerland). Powders were fed into the plasma stream by a 10-Twin-system (Plasma-Technik AG, Switzerland) during spraying. Spraying parameters were shown in Table 1.

The coating was deposited on an aluminum plate of dimensions 6 cm  $\times$  8 cm  $\times$  0.3 cm. Prior to spraying, the substrate was grit-blasted with alumina grits. During spraying, the substrate was cooled with high-pressure air at the back of substrate. A robot (ABB, Sweden) was employed to move the spray torch for a uniform and reproducible deposition. After deposition, the substrates were dissolved by sodium hydroxide (NaOH) solutions to obtain freestanding specimens.

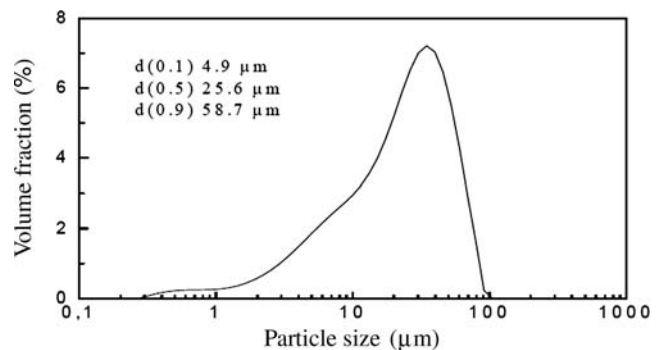


**Fig. 2** Size distributions of the YSZ powders used

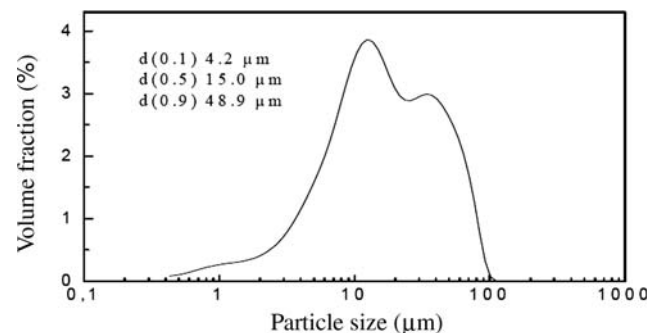


**Fig. 3** Size distributions of the LSM powders used

**Table 1** Spraying parameters used for deposition of LSM coating

|                                      | Value |
|--------------------------------------|-------|
| Current, A                           | 500   |
| Power, kW                            | 25    |
| Primary gas (Ar, SLPM)               | 26    |
| Secondary gas ( $\text{H}_2$ , SLPM) | 6     |
| Carrier gas (Ar, SLPM)               | 3.6   |
| Spray distance, mm/s                 | 100   |
| Gun traverse speed, mm/s             | 400   |

### 2.3 Microstructure Characterization

The phase constitutions of both the starting powders and deposited coatings were characterized by X-ray diffraction analysis (D/max2400, RIGAKU, Japan) using Cu K $\alpha$  radiation. A  $2\theta$  scanning rate of  $10^\circ\text{C min}^{-1}$  was used during test. The polished and fractured cross-sectional microstructures of the APS coatings were examined by scanning electron microscopy (JSM-6360LV, JEOL, Japan) with energy disperse X-ray spectroscopy (EDX) capability.

### 2.4 Electrical Conductivity Measurement

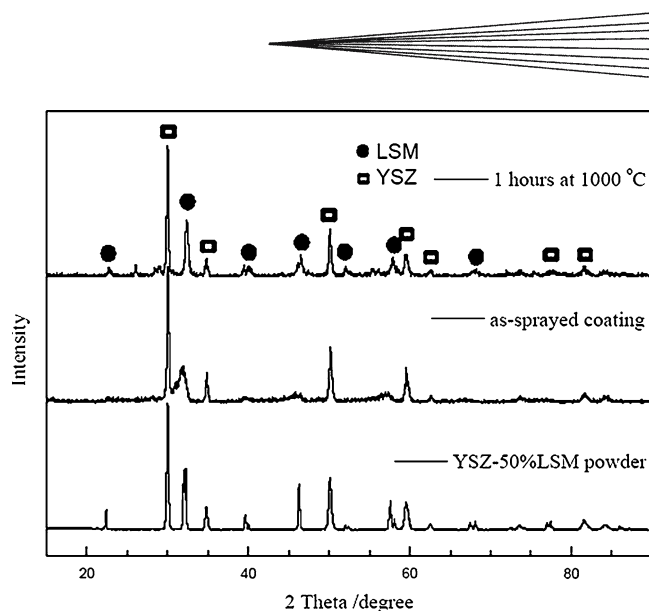
The circular freestanding YSZ/LSM coatings with a diameter of 15 mm were prepared for electrical conductivity measurement along the perpendicular direction to the coating surface. To ensure the measuring area of the circular planar sample, platinum glue was pasted on both sides of the sample with a specific effective area of  $1\text{ cm}^2$ . The pasted sample was dried at  $100^\circ\text{C}$  for 30 min and then heated to  $900^\circ\text{C}$  with a heating rate of  $5^\circ\text{C/min}$  and kept at  $900^\circ\text{C}$  for 30 min. According to the linear relation between current and potential difference, the resistivity and subsequently electrical conductivity were determined (Ref 18). Moreover, to investigate the influence of coating microstructure on the electrical conductivity of APS composite cathode coating, electrical conductivity along direction parallel to the coating surface was evaluated by a direct current (DC) four-terminal method in this study. The samples for this measurement had dimensions of  $35\text{ mm} \times 15\text{ mm} \times 0.8\text{ mm}$ . The specimens were pasted with four terminals platinum using platinum glue and heated as in the case of circular specimens.

## 3. Results and Discussion

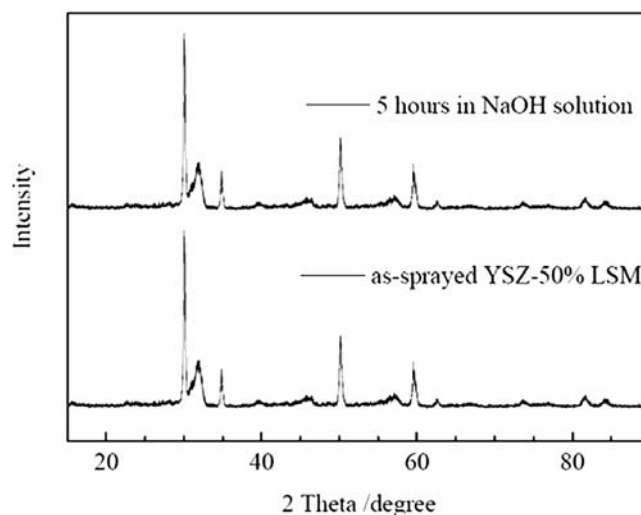
### 3.1 Microstructure of APS YSZ/LSM Composite Coating

Figure 4 shows the XRD patterns of the APS YSZ-50%LSM coating in comparison with the starting powder. XRD pattern indicated that the powder consisted of well-crystallized cubic zirconia phase and perovskite LSM. In the APS as-sprayed coating, YSZ could be clearly identified, whereas the LSM perovskite phase was weak. A thermal spray coating is generally deposited through the rapid splat cooling process. The high-cooling speed over  $10^5\text{ K/s}$  usually results in the formation of metastable phases in the coating (Ref 19).

The broadening of the XRD peaks of the perovskite LSM phase implies that fine crystalline grains were present in the as-sprayed composite coating. After a heat treatment at  $1000^\circ\text{C}$  for 1 h, the LSM perovskite phase became more pronounced due to the recrystallization, while the YSZ peaks remained unchanged. The XRD analysis suggests that the reaction between LSM and YSZ can be avoided during atmospheric plasma spray processing, because no strontium zirconates were recognized from the XRD pattern.



**Fig. 4** XRD patterns of the as-sprayed and heat-treated YSZ-50%LSM coatings in comparison with that of the starting powder



**Fig. 5** XRD patterns of the as-sprayed YSZ-50%LSM coatings in comparison with the NaOH treated coating

In order to examine the influence of sodium hydroxide solution on the property of the composite coating, the XRD pattern of a freestanding YSZ-50%LSM composite coating prepared by dissolution of the Al substrate using sodium hydroxide solution and the corresponding as-sprayed coating were conducted. Figure 5 shows that there is no observed difference between the two coatings. It indicated that dissolving the aluminum substrate with sodium hydroxide solution was a feasible method to get a free standing LSM/YSZ composite coating.

The examination of the polished cross-sectional microstructure clearly showed that a lamellar microstructure was presented in the LSM/YSZ coating as shown in Fig. 6. This fact means that the coating was deposited by sufficiently melted spray particles. The limited large voids observed on cross-section maybe resulted from spalling of

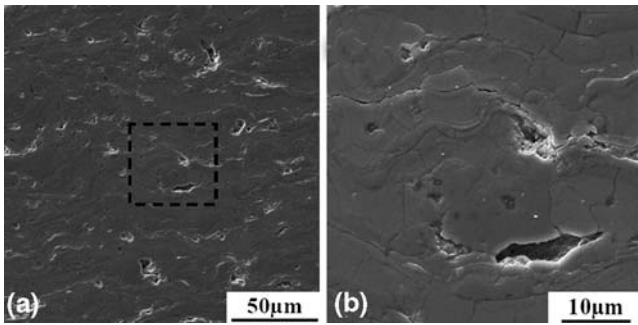


**Fig. 6** SEM polished cross-section microstructure of YSZ-50%YSZ coatings: (a) low magnification and (b) high magnification

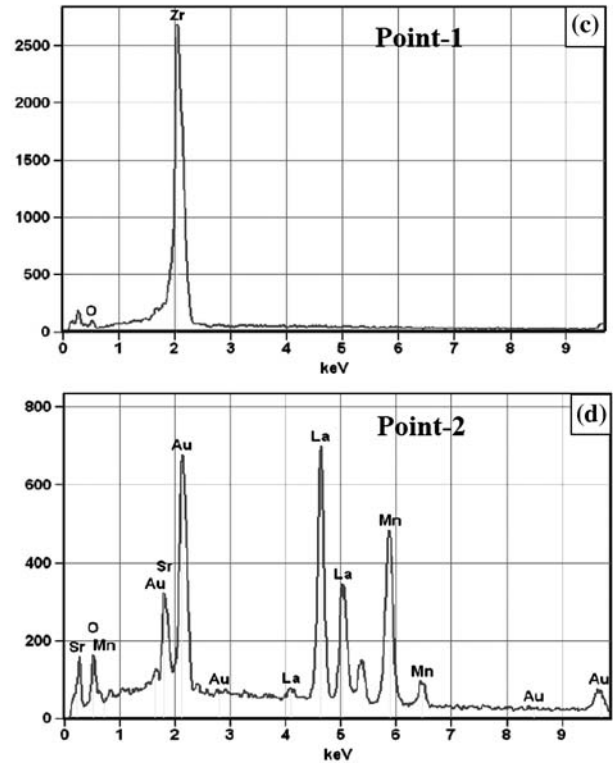
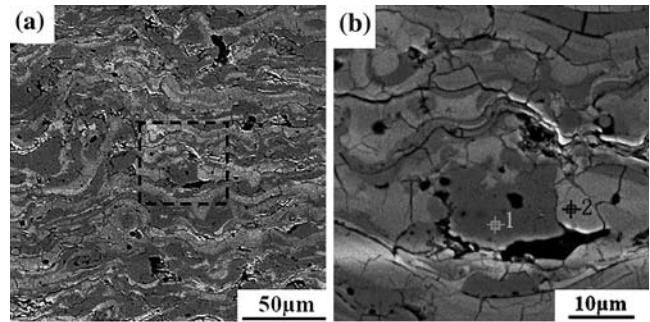
the coating during sample preparation. It can be observed that lamellar interface cracks and vertical cracks were presented in the polished cross-section, which were the inherent characteristic of APS ceramic coatings.

Figure 7(a), (b) shows the cross-sectional microstructure of the APS YSZ-50%LSM composite coating observed using backscattered electron (BSE) mode. There are two different colors in the coating corresponding to different phases. The dark grey phase was identified as YSZ while the light grey phase as LSM by EDX analysis as shown in Fig. 7(c), (d). It can be found that the coating was composed with well flattened YSZ and LSM splats. The YSZ splat and LSM splat were alternately accumulated and present evidence of lamellar feature.

### 3.2 Electrical Conductivity Measurement

Figure 8 shows the electrical conductivity of the three composite coatings along direction parallel to the coating surface measured at different temperatures. The electrical conductivity of the composite cathodes increased with the increase of measurement temperatures and the LSM ratio. The electrical conductivity of the YSZ-50%LSM sample increased from 2.17 to 3.60 S/cm when the test temperature increased from 500 to 900 °C while the values of the YSZ-60%LSM sample exhibited a slightly lower conductivity and ranged from 1.17 to 2.04 S/cm with the corresponding temperature increment. From the results reported by Ji et al. (Ref 20), YSZ-40%LSM sintered specimen showed an electrical conductivity from 15 to 31.6 S/cm at the same temperature range. The results obtained in this study are significant much lower than the above reported data.

The electrical conductivity of the three composite coatings along the perpendicular direction to the coating surface was also measured, as shown in Fig. 9. The electrical conductivity of the YSZ-50%LSM sample increased from 0.097 to 0.20 S/cm when the test temperature increased from 500 to 900 °C while the values of the YSZ-40%LSM sample exhibited slightly lower values ranging from 0.062 to 0.153 S/cm. Compared with the parallel electrical conductivity, the perpendicular value is only less than one tenth of that along the parallel direction. This phenomenon will be discussed in the following section.



**Fig. 7** SEM (BSE) polished cross-section microstructure of YSZ-50%LSM coatings: (a) low magnification, (b) high magnification, (c) EDX analysis of point 1, and (d) EDX analysis of point 2

The activation energy ( $E_a$ ) was calculated from the slopes of the linearly fitted lines according  $\log(\sigma T)$  and  $1/T$ . The activation energy of the coating along the parallel direction was about 0.80-0.83 eV in the temperature range, while it increased to 1.05-1.13 eV along the perpendicular direction.

### 3.3 Correlation Between Coating Microstructure and Electrical Conductivity

Plasma-sprayed coatings usually present a lamellar structure. The porosity from several up to around 20% is usually presented in ceramic coatings (Ref 21). The porosity of coating depends significantly on spray conditions. The previous studies into the lamellar bonded interface revealed that only a very limited lamellar is

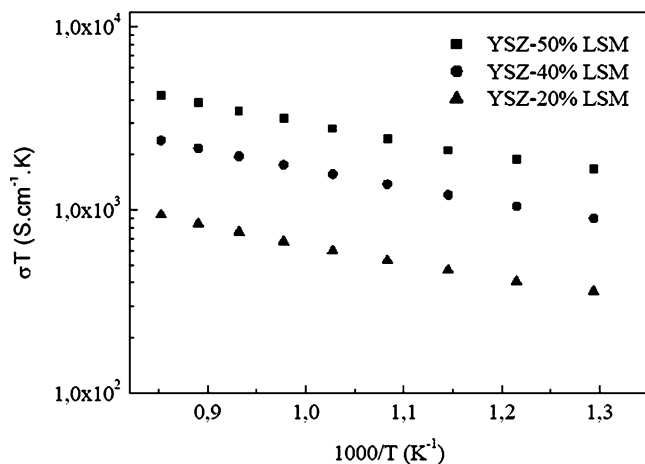


**Fig. 8**  $\sigma T$  vs.  $1/T$  plots of the electrical conductivity of the composite coating, along direction parallel to the coating surface

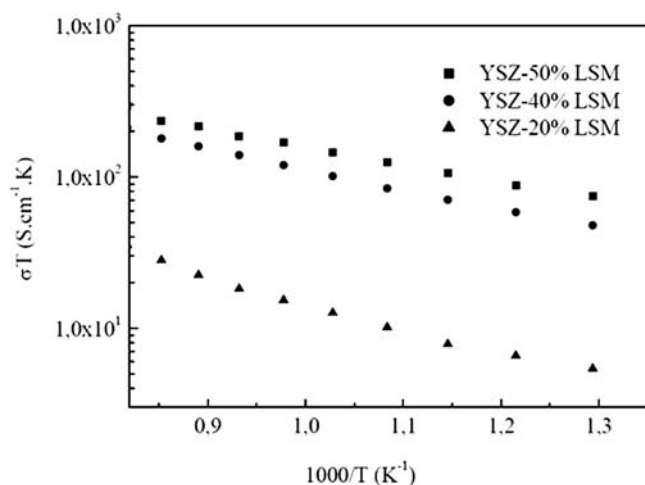


**Fig. 9**  $\sigma T$  vs.  $1/T$  plots of the electrical conductivity of the composite coating, along direction perpendicular to the coating surface

bonded together. The non-bonded interface exceeds two-thirds of the total apparent interface (Ref 22, 23).

Owing to the lamellar structural feature with limited interface bonding, electrical conductivity is much less than that of identical bulk material, which has been confirmed by our previous study (Ref 14, 18). Moreover, APS coating obviously presents anisotropy in electrical conductivity. The previous (Ref 14, 18, 24) studies revealed that the electrical conductivity of ceramic coating along the perpendicular direction to the coating surface was one-fifth to one-third of that of corresponding bulk materials. The electrical conductivity along the direction parallel to the surface is higher than that perpendicular to the surface. As depicted in our previous study (Ref 24), the electrical conductivity of APS YSZ coatings, along the parallel direction, can reach one-half of that of the corresponding bulk materials.

In this study, the coating was deposited with two different property materials. LSM bulk material exhibits a high-electronic conductivity of about 160-210 S/cm at 1000 °C while YSZ bulk material only has an ionic conductivity of 0.14-0.16 S/cm and no electronic conductivity. As a result, YSZ phase shows much lower electrical conductivity than that of LSM and interrupt the conduction of LSM and consequently increase the composite coating resistance. Moreover, the conduction of current will be interrupted by the non-bonded interface along direction parallel to surface and by vertical cracks along the parallel direction, which lead to a much lower electrical conductivity than that of the sintered bulk materials.

The activation energy of the coating along the parallel direction was about 0.80-0.83 eV at the temperature range of 500-900°C, while it increased to about 1.05-1.13 eV along the perpendicular direction at the same temperature range. As reported in our previous study (Ref 14, 24), the activation energy was only about 0.15 eV for pure LSM coating and 0.85-1.15 eV for YSZ coating, dependant on the temperature range. This fact implies that the conduction property of the composite coating was strongly influenced by YSZ phase.

#### 4. Conclusions

The microstructure and electrical conductivity of YSZ/LSM composite cathode materials prepared by APS process were investigated in this study. From XRD patterns of the APS YSZ/LSM composite cathode coatings, YSZ could be clearly identified, whereas the LSM perovskite peaks were weak. After a heat treatment at 1000 °C for 1 h, the LSM perovskite phase became more pronounced due to the recrystallization. From the SEM observation of the cross-section microstructure with EDX analysis, it can be found that the cathode coating was composed with alternative layering of well flattened YSZ and LSM splats.

The electrical conductivity of YSZ-50%LSM coatings changed from 2.17 to 3.60 S/cm along the parallel direction and from 0.097 to 0.20 S/cm along the perpendicular direction when the temperature changed from 500 to 900 °C. Significant anisotropy in the electrical conductivity was clearly observed. The anisotropy of the electrical conductivity is attributed to the different conductivity phase in the coating and the APS coating structure characteristics. The electrical conductivity of the composite cathode was increased with LSM content in the coating. The activation energy of the coating along both the two directions implies that the electrical conductivity of the composite was strongly influenced by the YSZ phase.

#### Acknowledgments

This work was financially supported by the French Ministry of Research (Program APURoute, No.:04F364). One of the authors (C. Zhang) wishes to thank the cotutors scholarship of French Government (Bourse du Gouvernement Français pour les cotutelles de thèse).

Authors are grateful to Wei Zhou of Xi'an Jiaotong University for his assistance of electrical conductivity measurement.

## References

1. M. Backhaus-Ricoult, Interface Chemistry in LSM-YSZ Composite SOFC Cathodes, *Solid State Ionics*, 2006, **177**, p 2195-2200
2. Peña-Martínez, D. Marrero-López, J.C. Ruiz-Morales, B.E. Buegler, P. Núñez, and L.J. Gauckler, Fuel Cell Studies of Perovskite-type Materials for IT-SOFC, *J. Power Sources*, 2006, **159**, p 914-921
3. I. Antepara, I. Villarreal, L.M. Rodríguez-Martínez, N. Lencanda, U. Castro, and A. Laresgoiti, Evaluation of Ferritic Steels for Use as Interconnects and Porous Metal Supports in IT-SOFCs, *J. Power Sources*, 2005, **151**, p 103-107
4. A. Skowron, P. Huang, and A. Petric, Structural Study of  $\text{La}_{0.8}\text{Sr}_{0.2}\text{Ga}_{0.85}\text{Mg}_{0.15}\text{O}_{2.825}$ , *J. Solid State Chem.*, 1999, **143**, p 202-209
5. J.W. Kim, A.V. Virkar, K.Z. Fung, K. Mehta, and S.C. Singhal, Low Temperature High Performance Anode Supported Solid Oxide Fuel Cells, *J. Electrochem. Soc.*, 1999, **146**, p 69-78
6. P.M. Figueiredo, J.R. Frade, and F.M.B. Marques, Performance of Composite  $\text{LaCoO}_3\text{-La}_2(\text{Zr,Y})_2\text{O}_7$  Cathodes, *Solid State Ionics*, 2000, **135**, p 463-467
7. B.C.H. Steele, K.M. Hori, and S. Uchino, Kinetic Parameters Influencing the Performance of IT-SOFC Composite Electrodes, *Solid State Ionics*, 2000, **135**, p 445-450
8. D. Herbstritt, A. Weber, and E. Ivers-Tiffée, Modelling and DC-Polarisation of a Three Dimensional Electrode/electrolyte Interface, *J. Euro. Ceram. Soc.*, 2001, **21**, p 1813-1816
9. S.Z. Wang, Y. Jiang, Y.H. Zhang, J.W. Yan, and W.H. Li, Promoting Effect of YSZ on the Electrochemical Performance of YSZ + LSM Composite Electrodes, *Solid State Ionics*, 1998, **113-115**, p 291-303
10. M.J. Jørgensen, S. Primdahl, C. Bagger, and M. Mogensen, Effect of Sintering Temperature on Microstructure and Performance of LSM-YSZ Composite Cathodes, *Solid State Ionics*, 2001, **139**, p 1-11
11. J.-P. Viricelle, C. Pijolat, B. Riviere, D. Rotureau, D. Briand, and N.F. de Rooij, Compatibility of Screen-printing Technology with Micro-hotplate for Gas Sensor and Solid Oxide Micro Fuel Cell Development, *Sensor Actuat. B: Chem.*, 2006, **118**, p 263-268
12. J.A.M. Van Roosmalen and E.H.P. Cordfunke, Chemical Reactivity and Interdiffusion of  $(\text{La,Sr})\text{MnO}_3$  and  $(\text{Zr,Y})\text{O}_2$  Solid Oxide Fuel Cell Cathode and Electrolyte Materials, *Solid State Ionics*, 1992, **52**, p 303-312
13. D.P. Lim, D.S. Lim, J.S. Oh, and I.W. Lyo, Influence of Post-treatments on the Contact Resistance of Plasma-sprayed  $\text{La}_{0.8}\text{Sr}_{0.2}\text{MnO}_3$  Coating on SOFC Metallic Interconnector, *Surf. Coat. Technol.*, 2005, **200**, p 1248-1251
14. C.-J. Li, C.-X. Li, and M. Wang, Effect of Spray Parameters on the Electrical Conductivity of Plasma-Sprayed  $\text{La}_{1-x}\text{Sr}_x\text{MnO}_3$  Coating for the Cathode of SOFCs, *Surf. Coat. Technol.*, 2005, **198**, p 278-282
15. S. Rambert, A.J. McEvoy, and K. Barthel, Composite Ceramic Fuel Cell Fabricated by Vacuum Plasma Spraying, *J. Eur. Ceram. Soc.*, 1999, **19**, p 921-923
16. D. Hathiramani, A. Mobeen, W. Fischer, P. Lersch, D. Sebold, R. Vaßen, D. Stöver, and R.J. Damani, Simultaneous Deposition of LSM and YSZ for SOFC Cathode Functional Layers by an APS Process, *Thermal Spray 2005: Explore its Surface Potential*, E. Lugscheider, Ed., May 2-4, 2005 (Basel, Switzerland), DVS, 2005, p 584-589
17. B.D. White, O. Kesler, N. Ben-Oved, and A. Burgess, Preparation of an SOFC LSM/YSZ Composite Cathode by Air Plasma Spraying, *Thermal Spray 2006: Building on 100 Years of Success*, B.R. Marple, M.M. Hyland, Y.C. Lau, R.S. Lima, and J. Voyer, Ed., May 15-18, 2006 (Seattle, WA), ASM International, Materials Park, OH, 2006
18. C. Zhang, H. Liao, W.-Y. Li, G. Zhang, C. Coddet, C.-J. Li, C.-X. Li, and X.-J. Ning, Characterization of YSZ SOFC Electrolyte Deposited by Atmospheric Plasma Spraying and Low Pressure Plasma Spraying, *J. Therm. Spray Technol.*, 2006, **15**(4), p 598-603
19. R. McPherson, The Enthalpy of Formation of Aluminium Titanate, *J. Mater. Sci.*, 1973, **8**, p 851-858
20. Y. Ji, J.A. Kilner, and M.F. Carolan, Electrical Properties and Oxygen Diffusion in Yttria-stabilised Zirconia (YSZ)- $\text{La}_{0.8}\text{Sr}_{0.2}\text{MnO}_3$  (LSM) Composites, *Solid State Ionics*, 2005, **176**, p 937-943
21. C.-J. Li, A. Ohmori, and R. McPherson, The Relationship between Microstructure and Young's Modulus of Thermally Sprayed Ceramic Coatings, *J. Mater. Sci.*, 1997, **32**, p 997-1004
22. A. Ohmori and C.-J. Li, Quantitative Characterization of the Structure of Plasma Sprayed  $\text{Al}_2\text{O}_3$  Coating by Using Copper Electroplating, *Thin Solid Films*, 1991, **201**, p 241-252
23. C.-J. Li and A. Ohmori, Relationship Between the Structure and Properties of Thermally Sprayed Coatings, *J. Therm. Spray Technol.*, 2002, **11**, p 365-374
24. C. Zhang, C.-J. Li, G. Zhang, X.-J. Ning, C.-X. Li, H. Liao, and C. Coddet, Ionic Conductivity and its Temperature Dependence of Atmospheric Plasma Sprayed Yttria Stabilized Zirconia Electrolyte, *Mater. Sci. Eng. B*, 2006, **137**, p 24-30